PNAS
www.pnas.org

Supplementary Information for

MicroRNA-dependent inhibition of PFN2 orchestrates ERK activation and pluripotent state transitions by regulating endocytosis

Carolyn Sangokoya and Robert Blelloch

Robert Blelloch
Email: robert.blelloch@ucsf.edu

This PDF file includes:

Supplementary Materials and Methods
Figures S1 to S6
Tables S1 to S2

www.pnas.org/cgi/doi/10.1073/pnas.2002750117

Supplementary Materials and Methods

Generation of PFN2 ESC mutant lines by CRISPR-CAS9 gene editing

Each guide RNA was cloned into a plasmid containing Cas9-GFP (OriGene plasmid GE100018, Rockville, MD). Paired guide-RNA plasmids were transfected into ESCs using FUGENE 6 (Roche) transfection reagent following the manufacturer's protocol. The next day, GFP positive ESCs were sorted and plated at single-cell density onto gelatinized plates. Individual clones were genotyped for shifts in PCR product size in both alleles, and the resulting products were gel extracted and verified by Sanger sequencing. Positive clones were expanded and the absence of PFN2 protein was confirmed by western blot. *Pfn2* mutant *Dgcr8*-KO ESC lines with disruptions in the PFN2-Dynamin interaction site at PFN2 serine-138 (S138) were generated by single guide RNA designed against this site in exon 3 of *Pfn2*, with processing as above. Guide sequences are listed in SI Appendix, Table S2.

Endosomal uptake assays

Cells were serum-starved in HBSS + 1% BSA for 30 minutes at 37°C, then washed and resuspended with 150 µg/ml pHrodo Red conjugated transferrin or 80 µg/ml pHrodo Red conjugated 10000 MW dextran (Thermo Fisher Scientific) for 20 min at 4°C. Media was quickly added to the cells before incubation at 37°C, with one sample left at 4°C as an internal control. After indicated internalization times, cells were quickly moved back to 4°C, washed with cold PBS, and prepared for analysis by flow cytometry using the BD LSR II Flow Cytometer System (BD Biosciences).

Immunoblot analysis

For immunodetection, immunoblots were incubated overnight at 4 °C with primary antibodies diluted in Intercept blocking solution (Licor) against alpha-tubulin at 1:3500 dilution (Sigma, T6074), profilin-2 at 1:700 dilution (BosterBio, PA2162), Phospho-p44/42 Erk1/2 Thr202/Tyr204 at 1:1000 dilution (Cell Signaling Technology, 4370), and p44/42 Erk1/2 at 1:1000 dilution (Cell Signaling Technology, 4696). Secondary infrared-dye antibodies were used at 1:10,000. Blots were scanned on a Licor Odyssey Scanner (Licor). Protein levels were quantified using ImageJ (http://rsb.info.nih.gov/ij/), and statistical calculations performed using at least 3 biological replicates. All unprocessed western blots are shown in SI Appendix, Fig. S6).

Quantitative real-time PCR

RNA was DNase-treated using amplification grade DNaseI (Sigma). For qRT–PCR of mRNAs, DNase-treated samples were reverse-transcribed using the Maxima first-strand cDNA synthesis system (Thermo Scientific). Real-time quantitative PCR for mRNA was conducted with SYBR

Green PCR master mix (Applied Biosystems) and performed on an ABI 7900HT (Applied Biosystems) according to the manufacturers' protocols using primer sets listed in SI Appendix, Table S1.

Cell cycle analysis

For EdU incorporation and DNA content analysis, cells were pulsed with 10 μM EdU (Life Technologies, Carlsbad, CA, USA) for 2 hours and subsequently stained according to manufacturer's protocol. FxCycle Violet was added to click-treated cells before flow cytometry acquisition on an LSRII (BD Biosciences) with FACS Diva software (BD). A total of 10,000 events were collected for cell cycle analysis per sample. FlowJo software was used to process the data and determine the percentage of sample cells in each cell-cycle phase (FlowJo).

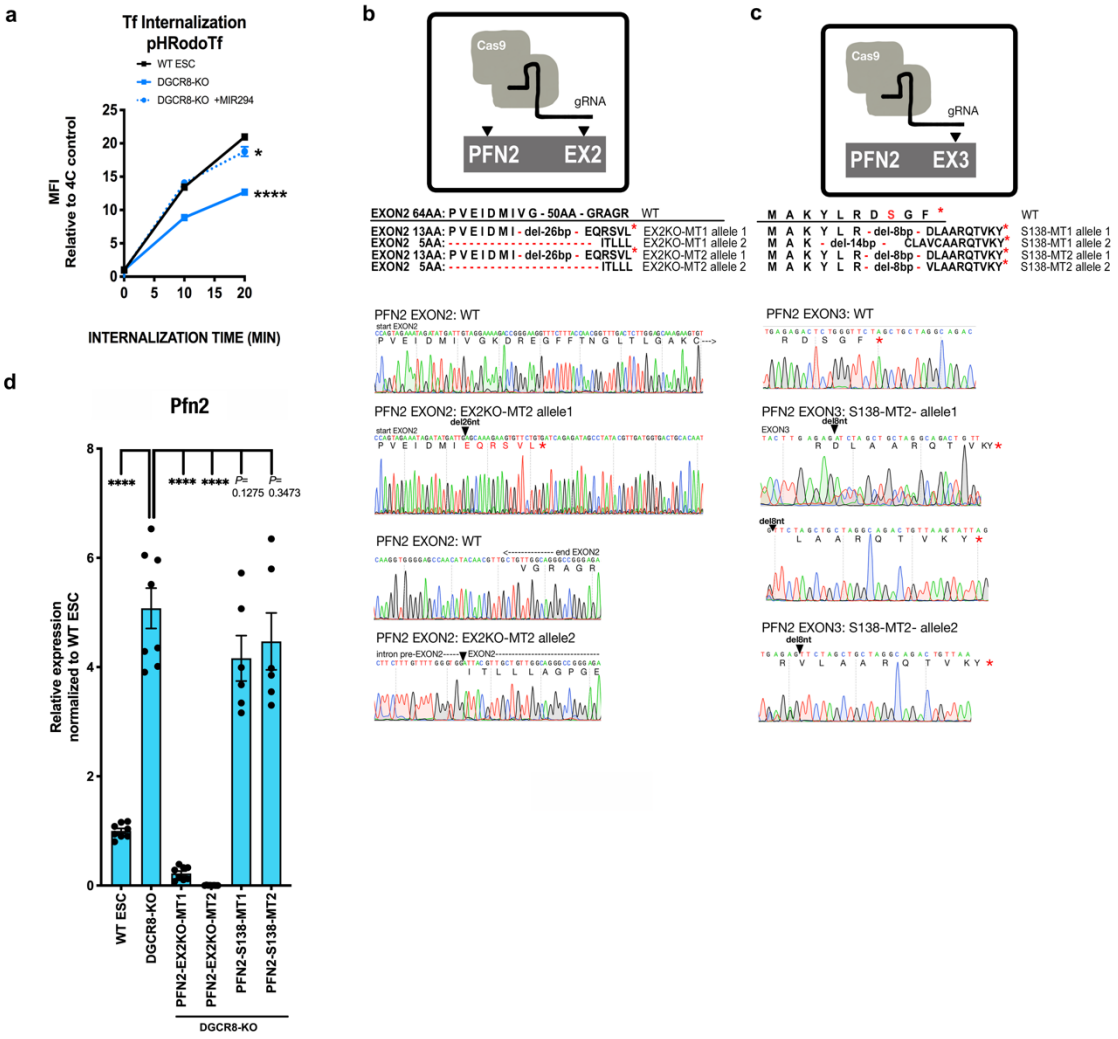

Fig. S1. (supplemental to Figure 1) **(**a) pH-labeled transferrin endosomal uptake assay in wild-type (WT), *Dgcr8*-KO, and *Dgcr8*-KO + miR-294 addback ESCs over indicated times, measured by change in mean fluorescence intensity (MFI) relative to control. n = 4 independent experiments. Media: serum+LIF. Error bars represent s.e.m. *P < 0.05, ****P < 0.0001 (unpaired two-tailed t-test) (b-c) Sanger sequencing results showing mutations of the two biallelic mutant clones of (b) *Pfn2* exon 2 and (c) *Pfn2* exon 3 mutants used in experiments. (d) qRT-PCR analysis of *Pfn2* expression in wild-type (WT), *Dgcr8*-KO, *Pfn2* exon2 (*Pfn2* -EX2KO) *Pfn2*-KO mutants MT1 and MT2, and *Pfn2* exon3 (PFN2-S138) *Dgcr8*-KO mutants MT1 and MT2. n = at least 6 independent experiments. Error bars represent s.e.m. ****P < 0.0001 (unpaired two-tailed t-test).

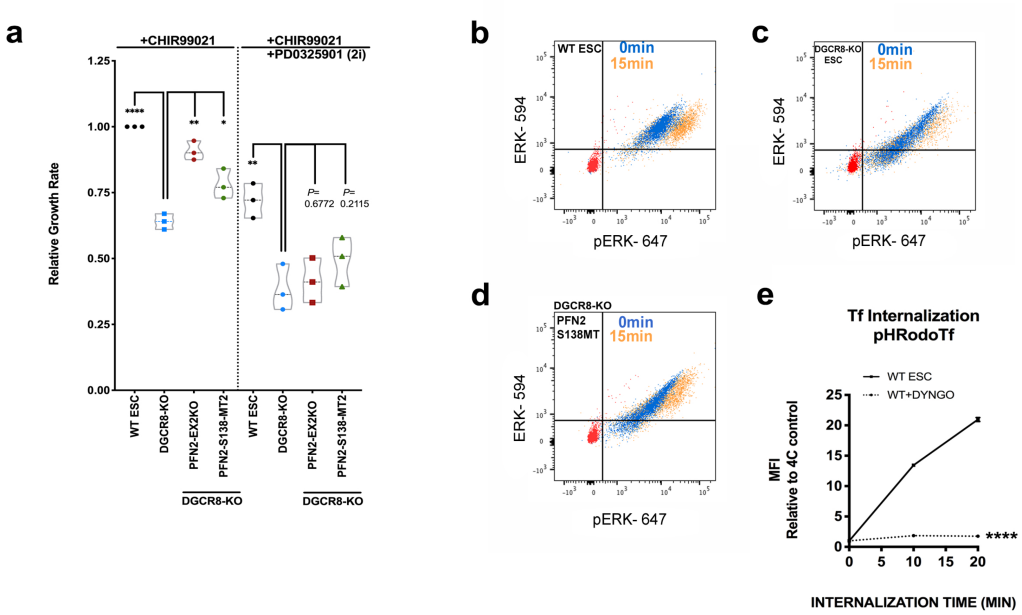

Fig. S2. (supplemental to Figure 3) (a) Growth rates of indicated ESCs relative to wild-type (WT) ESCs under 1i (CHIR99021) vs. 2i (CHIR99021 + PD0325901 conditions. n = 3 independent experiments. Media: serum+LIF with additions as indicated. Data shown as median ± quartiles. ***P < 0.001, **P < 0.01 (unpaired two-tailed t-test). (b-d) Representative dot blots of source data for Fig 3e-g. (e) pH-labeled transferrin endosomal uptake assay in wild-type (WT) ESCs with and without added dynamin inhibition over indicated internalization times, measured by change in mean fluorescence intensity (MFI) relative to control. n = 4 independent experiments. Error bars represent s.e.m. ****P < 0.0001 (unpaired two-tailed t-test)

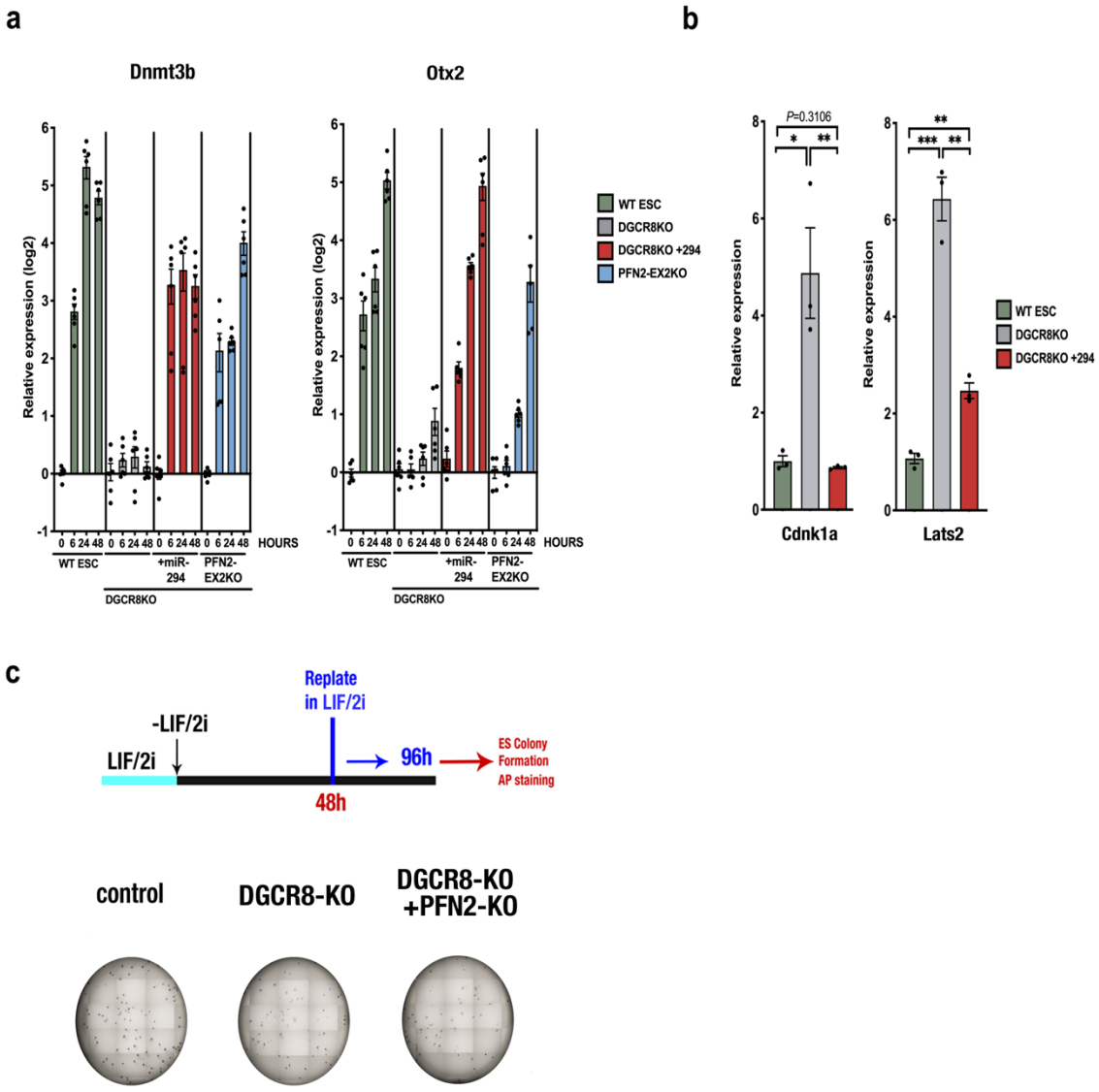

Fig. S3. (supplemental to Figure 4) (a) qRT-PCR analysis of *Lats2* and *Cdkn1a* expression in wild-type (WT), *Dgcr8*-KO, *Dgcr8*-KO with addback of miR-294 mimic (+294) or PFN2-depletion (*Pfn2*-EX2KO) ESCs under naïve conditions n=3 independent experiments. Error bars represent s.e.m. ***P < 0.001, **P < 0.01, *P < 0.05 (unpaired two-tailed t-test). (b) qRT-PCR analysis of EpiLC markers *Otx2* and *Dnmt3b* expression at indicated time points over ESC to EpiLC transition in wild-type (WT), Dgcr8-KO, Dgcr8-KO with addback of miR-294 mimic (+294) or *Pfn2*-EX2KO (in *Dgcr8*-KO background) ESCs n=3 independent experiments. Error bars represent s.e.m. ****P < 0.0001 (unpaired two-tailed t-test). (c) Top panel, replating assay schematic. Bottom panel, representative wells of indicated samples after completion of replating assay and AP staining.

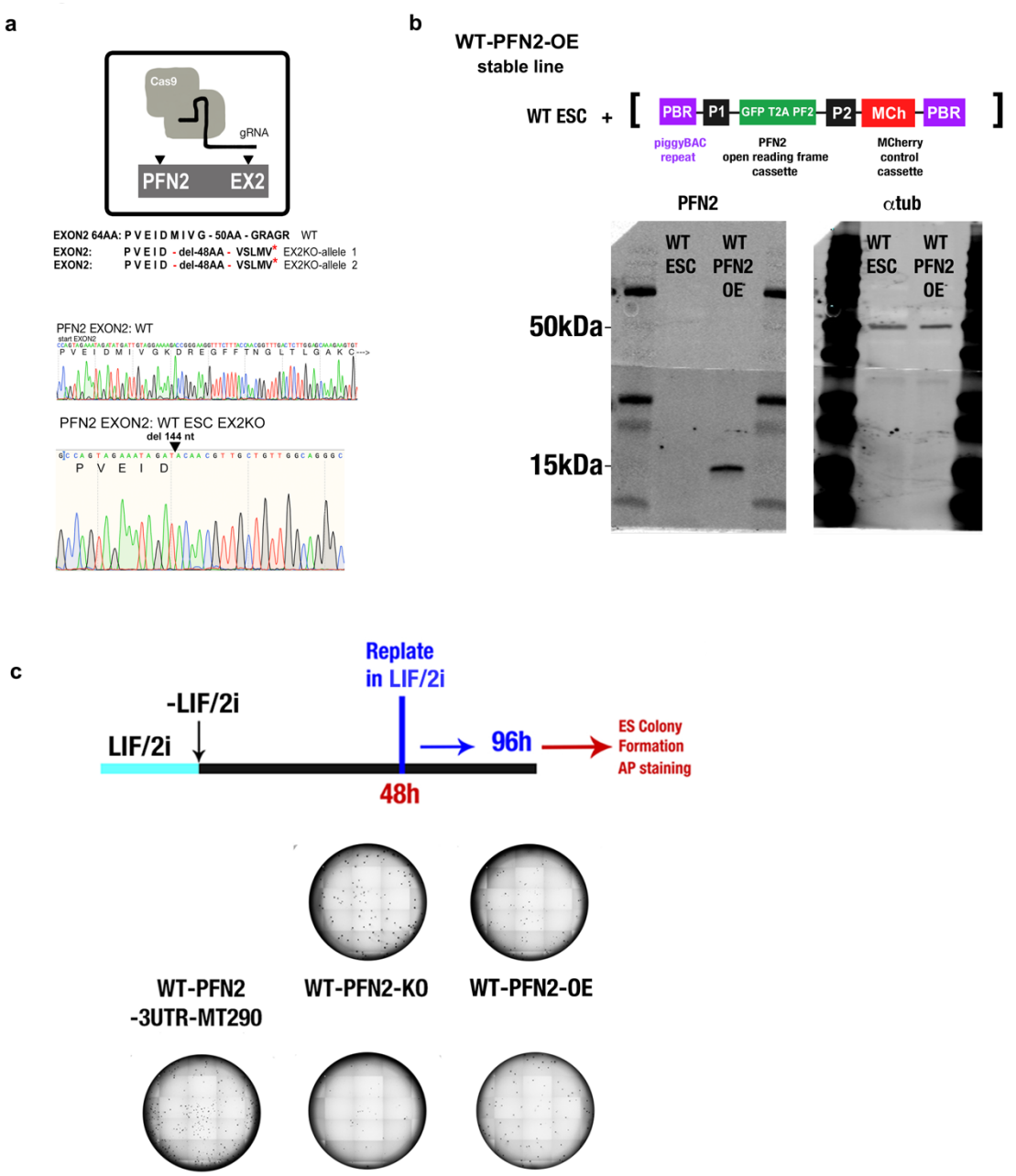

Fig. S4. (supplemental to Figure 6) (a) Schematic and Sanger sequencing results showing engineered CRISPR-based biallelic mutations of *Pfn2* exon 2 mutants used in experiments. (b) Top panel, schematic of construct used to generate stable line WT- *Pfn2*-OE in wild-type ESC background by integration using the piggyBac transposase system. Bottom panel, western blot confirmation of expression stable *Pfn2* expression in WT- *Pfn2*-OE line compared to wild-type ESC parental line. (c) Top panel, replating assay schematic. Bottom panel, representative wells of indicated samples after completion of replating assay and AP staining.

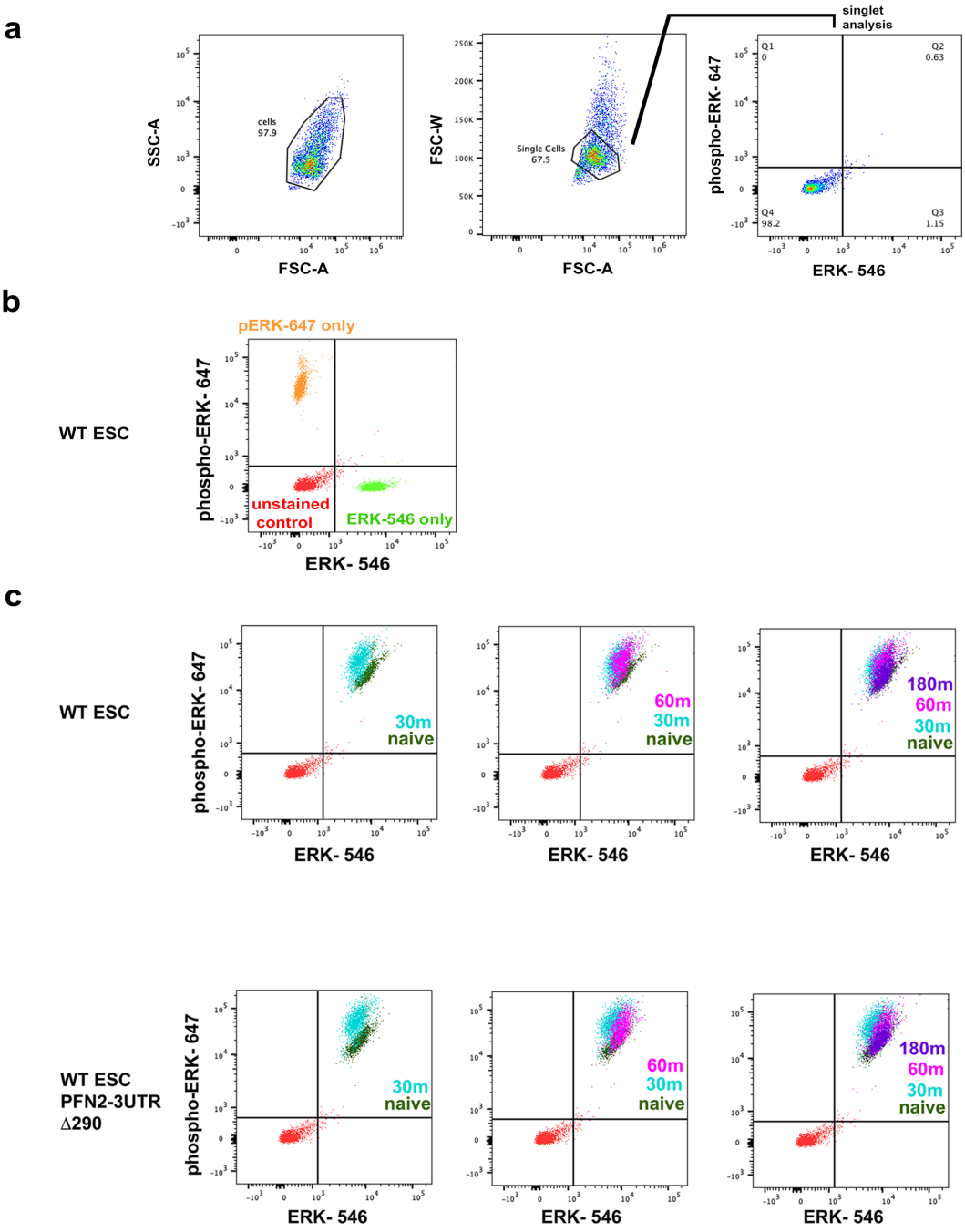

Fig. S5. (supplemental to Figure 6) (a) Figure exemplifying the gating strategies used. Briefly, viable cells were selected and cell debris excluded using the FSC vs SSC gate. We selected for singlets using FSC-width vs FSC-area gates. (b) Unstained cells of the same cell line or parental cell line were used as general negative controls for fluorescence. In the case of dual-color analysis, single-color controls were used to determine the boundaries between negative and single-color positive and dual-color positive cell populations. (c) Representative dot blots of source data for one replicate of ERK activation time course experiments summarized in Fig 6c.

Fig. 1a

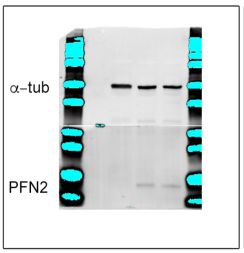

Fig. 1f

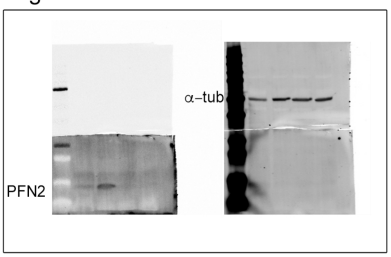

Fig. 1g

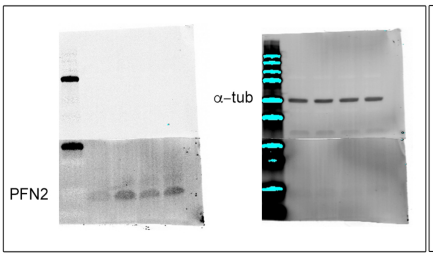

Fig. 3a

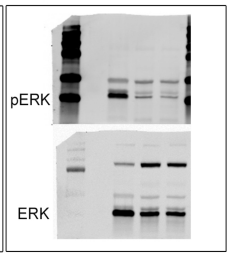

Fig. 3b

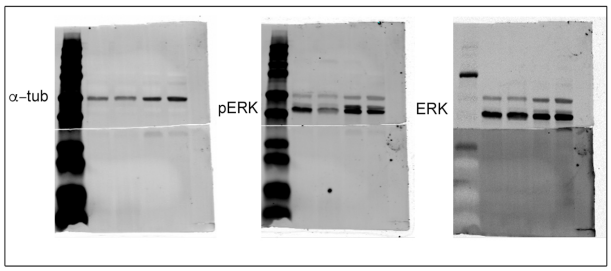

Fig. 3c

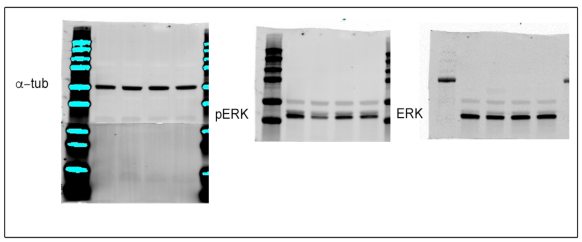

Fig. 5a & Fig. 7a

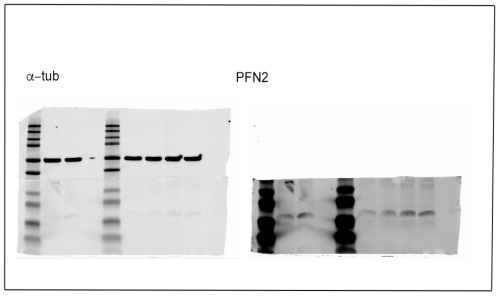

Fig. 5h

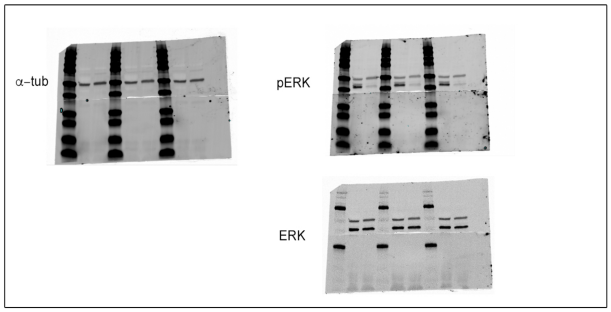

Fig. S6. Unprocessed western blots from indicated main text figures.

Table S1. Primers used for RT-qPCR analysis.

Gene	Forward	Reverse
Pfn2	TGTAGGAAAAGACCGGGAAGG	ACAGCAACGTTGTATGTTGGC
Rpl7	AGCGGATTGCCTTGACAGAT	AACTTGAAGGGCCACAGGAA
Cdkn1a	GTACTTCCTCTGCCCTGCTG	TCTGCGCTTGGAGTGATAGA
Lats2	AGCGTCGGTGTGATTCTCTT	TAGGGATATGCAGCGTGCTC
Esrrb	GAACACTCTCGCCTGGTAGG	CGCCTCCAGGTTCTCAATGT
Prdm14	TTCACGTCCATGAGAGGCAC	AGTACACGCACTGGTATGGC
Rex1	ATCGCTGTGGGCATTAGAGA	CGATCCTGCTTTCTTCTGTGT
Otx2	AAAGCAGAGGTGATCCGGTG	TCAGTCGCACAATCCACACA
Dnmt3b	CAGACAGGGCAAAAACCAGC	TTGGACACGTCCGTGTAGTG
Spry4	CAGGAAGGTAACGTCCGAGG	AGGTGGTTCACTGTAAGCCG
Dusp6	TGTCCCAGTTTTTCCCTGAG	CATCGTTCATGGACAGGTTG

Table S2. Guide RNA sequences used to generate CRISPR-based ESC mutant cell lines

Mutant cell line	Guides
DGCR8KO	ATTGTAGGAAAAGACCGGGA
PFN2EX2KO	CCAACAGCAACGTTGTATGT
DGCR8KO	
PFN2-S183MT	CAAAATACTTGAGAGACTCT
WT	
PFN2-3UTR-MT290	TCAGTGTCTTTTCAGCACTT
WT	ATTGTAGGAAAAGACCGGGA
PFN2EX2KO	CCAACAGCAACGTTGTATGT